

## Anodic oxidation of vanadium and properties of vanadium oxide films

This article has been downloaded from IOPscience. Please scroll down to see the full text article.

2004 J. Phys.: Condens. Matter 16 4013

(<http://iopscience.iop.org/0953-8984/16/23/018>)

View [the table of contents for this issue](#), or go to the [journal homepage](#) for more

Download details:

IP Address: 129.252.86.83

The article was downloaded on 27/05/2010 at 15:20

Please note that [terms and conditions apply](#).

# Anodic oxidation of vanadium and properties of vanadium oxide films

G B Stefanovich, A L Pergament, A A Velichko and L A Stefanovich

Research and Education Centre 'Plasma', Physics and Technology Department, Petrozavodsk State University, 185640 Petrozavodsk, Russia

E-mail: aperg@psu.karelia.ru

Received 6 February 2004

Published 28 May 2004

Online at [stacks.iop.org/JPhysCM/16/4013](http://stacks.iop.org/JPhysCM/16/4013)

DOI: 10.1088/0953-8984/16/23/018

## Abstract

Thin films of amorphous vanadium oxide have been prepared by electrochemical anodic oxidation. The phase composition of anodic films on vanadium has been shown to depend on the oxidation conditions (electrolyte composition, oxidation current, and time), and the stoichiometry can be controlled from  $\text{VO}_2$  to  $\text{V}_2\text{O}_5$ . Physical properties of the oxide films, including the metal–insulator transition in amorphous  $\text{VO}_2$ , are studied. In addition, it is shown that non-equilibrium electrochemical oxidation leads to the formation of metastable vanadium oxides with extremely high sensitivity to laser ( $\sim 1 \text{ mJ cm}^{-2}$ ) and electron-beam ( $\sim 10 \mu\text{C cm}^{-2}$ ) irradiation. Such films are of considerable technical interest, particularly because of potential applications as an efficient resist material for both photonolithography and electron-beam nanolithography.

## 1. Introduction

Electrochemical techniques provide simple and inexpensive alternative routes to the synthesis of thin films and special coatings, nanostructured materials, and metastable phases [1]. Anodic oxidation allows for preparation of oxide films on a number of metals and semiconductors, such as: aluminium; Ta, Nb, and many other transition metals; silicon; A3B5 semiconductors [2]. Due to their large variety of properties, passive anodic oxide films (AOFs) play an important role in various technical applications in surface protection, microsystems and nanosystems, and electrocatalysis [3], and as electrochromic [4] and photosensitive [5] materials, dielectrics in electrolytic capacitors [2], and gate insulators in MIS devices [6].

Anodic oxides of transition metals are worthy of special mention both due to their wide technical applications and because of interesting physical properties. In particular, since the AOFs are usually amorphous [1–3], they are receiving increased attention because of general interest in the disordered state, especially in the problem of an interplay between disorder

and electron interactions in the strongly correlated systems [7]. Strong electron–electron and electron–phonon correlations in the compounds of transition metals are associated with the specific behaviour of d electrons. It is now commonly accepted that strong correlation effects are responsible for the unique properties of such materials as high- $T_c$  superconductors, manganites with colossal magnetoresistance, and materials with metal–insulator transitions (MITs) [8]. For example, the MIT in disordered VO<sub>2</sub> has been previously studied in [9].

On the other hand, due to the existence of unfilled d shells, transition metals possess a set of valence states and, in compounds with oxygen, form a number of oxides. Therefore, AOFs on transition metals can consist of different oxide phases [7, 10]. In particular, the phase composition of anodic oxides on vanadium has been identified by different authors as either V<sub>2</sub>O<sub>5</sub> [4, 10, 11] or VO<sub>2</sub> [9, 12, 13], or as a mixture of V<sub>2</sub>O<sub>5</sub> and lower oxides [10, 14–16]. Also, passive films composed of barium vanadate [14] or vanadophosphate [17] can be obtained by anodization of V in aqueous solutions in some cases. Earlier, in the work [7], it was shown theoretically that the phase composition of vanadium anodic oxide depends on the oxidation conditions and electrolyte composition. In the present paper we will investigate this problem in more detail experimentally.

When vanadium is anodized in an aqueous solution, the vanadium oxide film tends to dissolve in the solution as vanadyl ions [12, 14, 18]. Therefore, because of the solubility of vanadium oxides in water, non-aqueous solutions are necessary for obtaining uniform oxide films on vanadium by anodization. Glacial acetic acid containing small additions of water and sodium tetraborate has been found most suitable for the anodization of vanadium [13, 19]. The total amount of Na<sub>2</sub>B<sub>4</sub>O<sub>7</sub> present in the solution was not considered to be critical; however, the film growth was observed to be sensitive to the water–borate ratio [13]. Breakdown of the oxide film was observed at applied potentials above ~25 V. Later studies found that smaller amounts of water in the acetic acid solution would still yield good oxide films. Ellis *et al* [19] used an acetic acid solution containing only enough water to dissolve all the sodium tetraborate. Therefore the water–borate ratio may not be as important as previously thought. When the water content was reduced, formation voltages of up to 100 V yielded reproducible films [12, 20].

The source of the oxygen in the film is important in determining the mechanism of formation of the film [12]. Keil and Salomon [13] have suggested that the oxygen in the oxide film is provided by the water in the anodizing solution. This was based upon the fact that no oxide film could be formed on the vanadium if water was not present regardless of the voltage or current density applied to the anode. However, the amount of water seems not to be very critical as long as a quantity sufficient to dissolve the sodium tetraborate is present. Other sources of the oxygen may be from the acetic acid itself or from Na<sub>2</sub>B<sub>4</sub>O<sub>7</sub>. Lewis and Perkins [12] have concluded that the tetraborate, not the water, acts as the source of the oxygen for the film. Pelleg [21] has found an acetone-based electrolyte (i.e. without acetic acid at all), containing Na<sub>2</sub>B<sub>4</sub>O<sub>7</sub> plus benzoic acid, in which anodic vanadium oxide films could be formed, but his interest was in microsectioning vanadium, not in growing oxide.

We thus conclude that vanadium, among other transition metals, possesses special and very interesting properties and can, for example, form the lower oxide (VO<sub>2</sub>) under anodic oxidation [7, 9]. That is why the process of anodic oxidation of vanadium has received much attention in the literature [4, 7, 9–21]. Nevertheless, in spite of these efforts, a number of problems—particularly the problem of phase composition—have not been definitively solved yet. Therefore, in the present work, we have studied the process of anodic oxidation of vanadium and the properties of oxide films. The primary goal of these studies is to elucidate a correlation between the preparation conditions and regimes and the electrolyte composition, on the one hand, and the properties and stoichiometry of the ensuing films, on the other hand. The potentialities of vanadium anodic oxides for applications in electronics and nanotechnologies are also discussed.

## 2. Experimental procedures

Both polished foils and vacuum deposited (by magnetron sputtering and electron-beam evaporation onto glass-ceramic and Si substrates) layers were used as the metal vanadium specimens for oxidation. The vanadium foil specimens were previously electropolished in a 40% H<sub>2</sub>SO<sub>4</sub> solution in ethanol at a current of approximately 0.5 A cm<sup>-2</sup>.

For anodic oxidation of vanadium the electrolyte was made up of 22 g of benzoic acid (C<sub>6</sub>H<sub>5</sub>COOH) and 2–50 ml of a saturated aqueous solution of borax (Na<sub>2</sub>B<sub>4</sub>O<sub>7</sub> × 10H<sub>2</sub>O) per 1 l of acetone [9, 22]. Salicylic (*o*-oxybenzoic) and gallic (trioxybenzoic) acids were also used instead of benzoic acid in some cases. The acetone-based electrolyte was chosen because of negligible dissolution of the films in this solution, unlike in the acetic acid-based electrolytes [21].

Anodization was carried out under both galvanostatic ( $I = \text{constant}$ ) and volstatic ( $V = \text{constant}$ ) conditions. A conventional glass three-electrode electrochemical cell was used with a stainless steel or nickel cathode and a platinum reference electrode. The electrolyte was not protected from air, and it was therefore changed after every 10–15 anodizations. The distance between the cathode and anode (vanadium sample) was maintained at 10 mm, and a typical sample surface area was 1–3 cm<sup>2</sup>. After anodization, the samples were immediately immersed into pure acetone, carefully rinsed there, and then rapidly dried in airflow or by a filter paper.

A constant formation current or voltage was maintained using a Keithley 227 power supply. The potential of the anode with respect to the Pt reference was measured with a digital voltmeter, the output of which was connected with a 'voltage versus time' recorder for the kinetics investigation.

The electrolyte composition was monitored by means of the pH and conductivity measurements using, respectively, a Model AR 20 pH meter and an ACCUMET AB30 conductivity meter.

The optical and electrical properties of the films were studied by standard techniques, including the four-probe conductivity method and optical spectrophotometry. Auger electron spectroscopy (AES) (Physical Electronics Industries, Inc.; 0.3% resolution), x-ray diffraction (XRD) structural analysis (DRON-4, Cu K $\alpha$  radiation), and scanning electron microscopy (SEM; Hitachi S-2300 with resolution down to ~10 nm) were used to identify the chemical composition, crystal structure and morphology of the materials. The thickness of the films was measured using the ellipsometry method [2–4, 9].

To get further important information on the properties of the vanadium AOF, experiments on laser and electron-beam modification of the vanadium anodic oxides were performed. These experiments were carried out using a YAG:Nd<sup>3+</sup> laser and an SEM-based nanopattern generation system (NPGS). Exposure doses were varied in the ranges from 0.1 to 100 mJ cm<sup>-2</sup> and 5 to 1000  $\mu\text{C cm}^{-2}$ , respectively. The sample preparation procedures, as well as some details of experimental and analytical techniques, have been described previously [5, 9, 22].

## 3. Results and discussion

### 3.1. Kinetics of oxidation

In a standard electrolyte system (with  $C = 40$  ml of borax per litre of acetone and with benzoic acid) vanadium can generate passive oxide films with uniform interference colours. The kinetics of oxidation of vanadium, shown in figure 1, is similar to that obtained for the typical 'valve' [2] metals, such as Ta or Nb. Under galvanostatic conditions, the voltage  $V$  approxi-

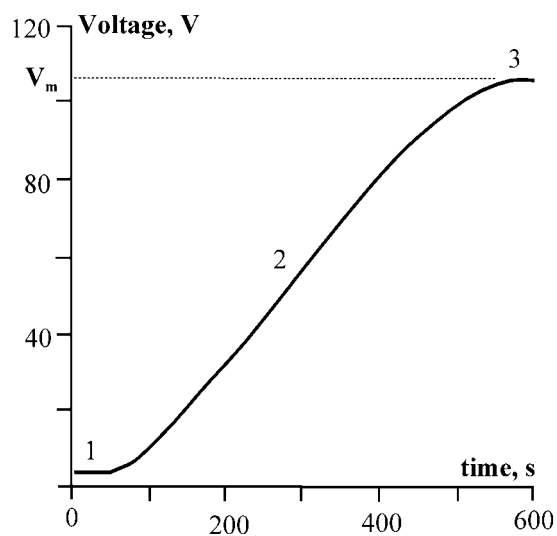


**Figure 1.** Kinetics of anodic oxidation of vanadium under galvanostatic conditions,  $j = 5 \text{ mA cm}^{-2}$ . Initial transient (1), linear (2), and dissolution commencement (3) regions are marked.

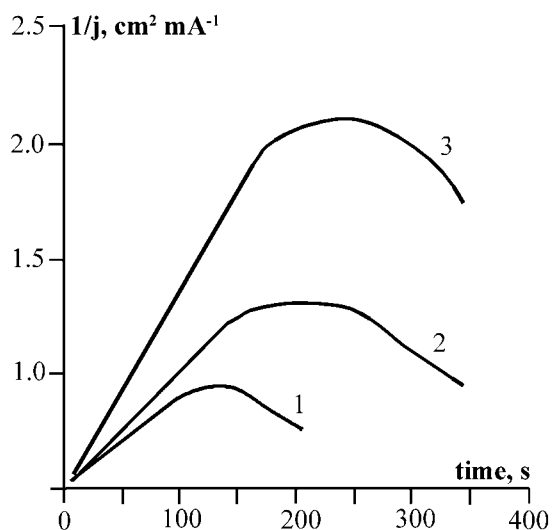


**Figure 2.** Reciprocal current density as a function of time under volstatic conditions, depending on the electrolyte composition and applied voltage: (1)  $V = 80 \text{ V}$ ,  $C = 40 \text{ ml}$  of borax per litre of acetone; (2)  $V = 80 \text{ V}$ ,  $C = 2 \text{ ml}$ ; (3)  $V = 40 \text{ V}$ ,  $C = 2 \text{ ml}$ .

mately linearly depends on the anodizing time  $t$ , except for the low voltage and high voltage regions (figure 1). Under volstatic conditions, the current density  $j$  is inversely proportional to time until a certain critical value  $t_m$  is reached (figure 2). After this, an increase of  $j$  (decrease of  $1/j$ ) commences. The maximum anodizing voltage  $V_m$  (see figure 1) is determined by the process of the active oxide dissolution [22], but not by the sparking (breakdown), as usually [2]. The dissolution is responsible also for the current increase at  $t > t_m$ . Films formed at a constant

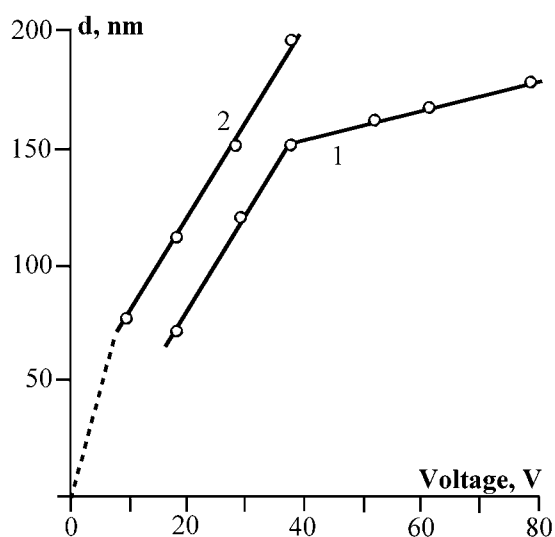


**Figure 3.** Thickness of anodic oxide films on vanadium as a function of anodizing voltage for (1) galvanostatic and (2) volstatic regimes.

voltage in the range 10–80 V for  $t < t_m$  (figure 2) had uniform interference colours. However, as the result of dissolution (i.e., for the samples anodized at  $V > V_m$  or  $t > t_m$ ) the colours of the films became inhomogeneous. The increase of the water concentration in the electrolyte led to growth of the dissolution rate; as the water content increased, both  $V_m$  and  $t_m$  decreased. The same effect was observed when the value of  $j$  (under galvanostatic conditions) was increased.

The dependences of the film thickness,  $d$ , on the anodizing voltage are presented in figure 3. A linear relationship between the film thickness and applied voltage is observed for the volstatic regime (2 in figure 3). This is quite usual for anodic oxidation of standard valve metals [2], and for vanadium as well [10, 12, 13, 21]. On the other hand, in the case of galvanostatic anodization (1 in figure 3), the dependence of  $d$  on  $V$  consists of two linear regions. We suppose that this is associated with the existence of a surface layer on metal vanadium, which is saturated by oxygen. This assumption is supported by the high solubility of oxygen in vanadium (up to 12 at.% [23]), and the ellipsometry measurements do reveal the existence of such a layer which forms during the vanadium substrate ageing in air. The growth rate  $dx/dV$  (i.e. the slope of the graphs of figure 3) changes suddenly at the transition from oxidation of this 'VO<sub>x</sub>' layer to oxidation of pure vanadium due to the change of the field strength,  $dV/dx$ . For volstatic anodization, the same change seems to take place at  $V < 10$  V (dashed line in figure 3).

From the data of figures 1 and 3, it is straightforward to calculate the efficiency (faradic yield) of the oxidation reaction,  $\eta$ . The film thickness is given by the expression [2]

$$d = \eta(jt\mu/2yF\rho), \quad (1)$$

where  $\mu$  and  $\rho$  are, respectively, the molecular weight and the density of oxide,  $F = 9.65 \times 10^4 \text{ C mol}^{-1}$ —the Faraday number, and  $2y$  is the reaction valency, i.e.  $y$  is the stoichiometric index of oxygen in the formula of the oxide. In our case, for VO<sub>2</sub>,  $\mu = 83 \text{ g mol}^{-1}$ ,  $\rho = 4.34 \text{ g cm}^{-3}$  [12, 24], and  $y = 2$ . For the anodizing voltage of, e.g., 40 V,  $t = 230 \text{ s}$  at  $j = 5 \text{ mA cm}^{-2}$  (from figure 1), and equation (1) yields, for  $\eta = 1$ ,  $d = 570 \text{ nm}$ , while the experimental value is  $d = 155 \text{ nm}$  for  $V = 40 \text{ V}$  (see figure 3, curve 1). Therefore,  $\eta = 155/570 = 0.27$ , that is, the oxidation efficiency is only 27%. This is accounted for by

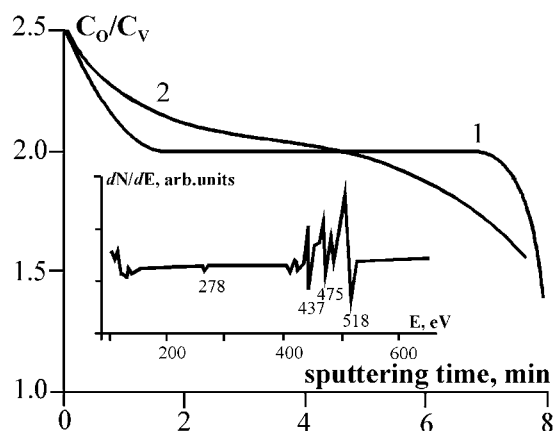


**Figure 4.** The thickness dependence of the oxygen to vanadium concentration ratio in the anodic oxide films on V grown in electrolytes with (1)  $C = 40$  ml and (2)  $C = 2$  ml. The values of  $C_O$  and  $C_V$  were obtained from AES (a typical Auger spectrum is shown as the inset) under sputtering by  $\text{Ar}^+$  ions, and the stripped oxide thickness is proportional to the sputtering time.

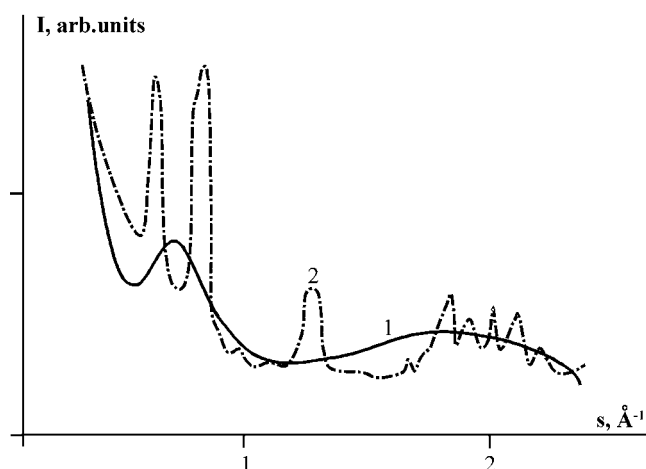
the fact that some other parallel reactions can occur preferentially to oxide growth [7]—namely, oxidation of the electrolyte components, anodic dissolution of the metal, and dissolution of the growing oxide. The latter process, in view of the aforesaid, seems to be predominant in the case of anodic oxidation of vanadium under the conditions described. In other cases, the value of  $\eta$  can be as high as almost 100% [13].

### 3.2. Properties of the anodic vanadium oxide films

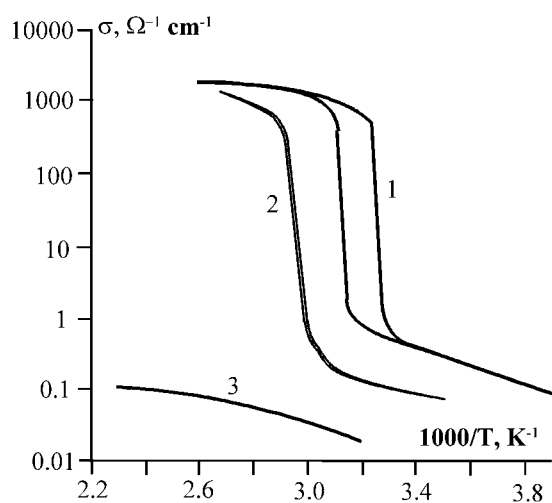
For compositional and stoichiometry analysis of anodized vanadium films, we used a combination of different analytical techniques including: AES; XRD and electron diffraction; UV, visible, and IR spectrophotometry [5, 9]. The composition and oxygen stoichiometry of the films were found to be strongly dependent on the sodium tetraborate aqueous solution (actually, water content) in the electrolyte.

Figure 4 shows the typical depth profiles of the oxygen content for two different anodic oxide films on vanadium. These results indicate that in AOF on vanadium, the vanadium dioxide layer can be made rather thick (curve 1 in figure 4) and only a very thin film near the outer boundary is close to the  $\text{V}_2\text{O}_5$  stoichiometry. Thus, it has been found that the compositions of anodic films on V are basically subject to the influence of such factors as the electrolyte composition (especially the content of the  $\text{Na}_2\text{B}_4\text{O}_7$  aqueous solution), as well as the anodizing voltage and current and time of the anodization process. This is in accordance with the predictions based on thermodynamic considerations. As was shown in [7], anodic films on Nb, Ti, Mo, and W must consist of the corresponding highest oxides of these metals, and  $\text{NbO}_2$ ,  $\text{Ti}_2\text{O}_3$ ,  $\text{MoO}_2$ , or  $\text{WO}_2$  layers are relatively thin, while the AOFs on vanadium may consist of, mainly, vanadium dioxide, and only a thin film near the outer boundary corresponds to the  $\text{V}_2\text{O}_5$  phase.

Vanadium anodic oxides are also of particular interest because of the MIT in  $\text{VO}_2$ . The point is that there is still no consensus as to the description of the driving mechanism of the transition: whether it is due to electron correlation effects or structural instabilities [8, 9, 25, 26]. It is apparent therefore that the investigation of the physical properties of amorphous  $\text{VO}_2$  is the most straightforward and effective way to clarify the mechanism of the MIT in this compound.



**Figure 5.** XRD patterns of (1) initial vanadium anodic oxide and (2) that same film subjected to laser radiation ( $\lambda = 1.06 \mu\text{m}$ ) with the energy  $E = 1.5 \text{ mJ cm}^{-2}$ .



**Figure 6.** Conductivity as a function of reciprocal temperature for amorphous vanadium dioxide film (1), polycrystalline  $\text{VO}_2$  film obtained by reactive magnetron sputtering (2), and amorphous vanadium pentoxide (3).

Summarizing the above-presented results, we conclude that vanadium dioxide can be obtained by anodic oxidation, and, as was already noted above, these films are of interest just because of the investigation of the MIT in structurally disordered  $\text{VO}_2$ . The experimental data on XRD (see figure 5, curve 1) show that the spectrum exhibits diffuse maxima typical for amorphous materials. The occurrence of the MIT in the amorphous  $\text{VO}_2$  films was indicated by an abrupt and considerable (although reversible) change in the conductivity at  $T = 310\text{--}330 \text{ K}$  (figure 6). This temperature practically coincides with the transition temperature for the MIT in  $\text{VO}_2$ ,  $T_t = 340 \text{ K}$  [8]. The importance of these results consists in the evidence that the metal–insulator transition in  $\text{VO}_2$  is preserved in the absence of long-range crystallographic order. This, in turn, suggests that electron–electron correlations play an important role in the transition



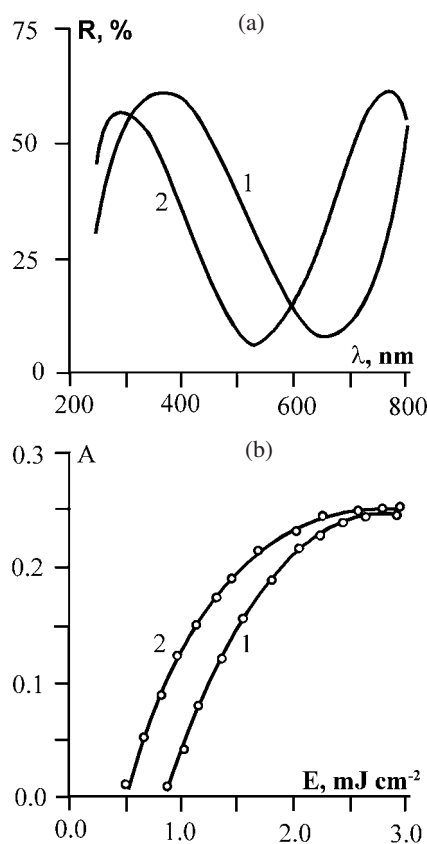


**Figure 7.** (a) Reflectance spectra of the initial (1) and laser treated at  $E = 1.5 \text{ mJ cm}^{-2}$  (2) vanadium anodic oxide. (b) Optical contrast  $A = |(R_1 - R_2)/(R_1 + R_2)|$  (measured at a certain wavelength  $\lambda'$ ) as a function of laser radiation energy ( $A \rightarrow 0$  at  $E = E_0$ ) for radiation with  $\lambda = 1.06 \mu\text{m}$  (1) and  $0.53 \mu\text{m}$  (2).

mechanism [9], and hence the MIT in  $\text{VO}_2$  is purely an electronic Mott transition, rather than a Peierls transition (for which, in the first approximation, a long-range order is necessary). The validity of this conclusion has been recently discussed in more detail in the work [25].

### 3.3. Modification of the properties of vanadium anodic oxide

It is known that transition metal oxides can undergo structural and phase transformations under the action of different external perturbations—heat treatment, electron and ion bombardment, laser radiation [5]. We therefore next investigated the effects of laser and e-beam irradiation on the properties of vanadium anodic oxide, and some results are presented below. Laser irradiation was performed using a  $Q$ -switched solid-state laser operated at wavelength  $1.06 \mu\text{m}$  with 15 ns pulse duration. Radiation with  $\lambda = 0.53$  and  $0.26 \mu\text{m}$  was also used during, respectively, second- and fourth-harmonic generation. Experiments on e-beam exposure were performed using a Hitachi S-2300 SEM with an NPGS system, with the following parameters: accelerating voltage 5–20 kV and current 40 pA to 1 nA.

First we measured the threshold energy,  $E_0$ , of the laser radiation required to produce the modification.  $E_0$  was determined by measuring the dependence of the optical contrast on the laser radiation energy (figure 7).

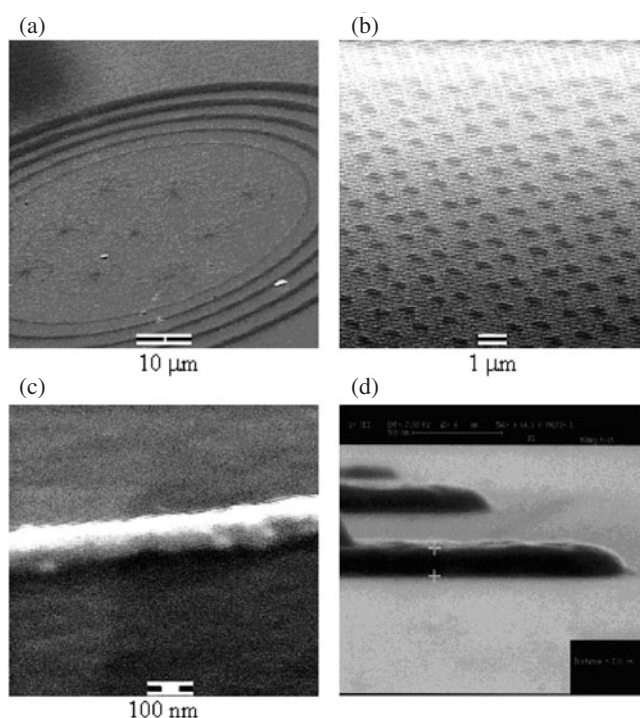


**Figure 8.** Vanadium oxide resist patterns on Si (after e-beam exposure at 15 kV and developing): (a) diffraction grating, (b) 'dots', and (c), (d) submicron lines obtained with the dose of  $175 \mu\text{C cm}^{-2}$ ; the height of the step (d) is 138 nm.

The values of  $E_0$  were measured to be 0.8 and  $0.5 \text{ mJ cm}^{-2}$  for  $\lambda = 1.06$  and  $0.53 \mu\text{m}$ , respectively (figure 7(b)). For ultra-violet ( $0.26 \mu\text{m}$  wavelength) radiation, it was established that  $E_0$  was of the order of that for 1.06 and  $0.53 \mu\text{m}$ , i.e.  $\sim 1 \text{ mJ cm}^{-2}$ . For e-beam modification, the threshold dose,  $D_0$ , was found to be  $\sim 10 \mu\text{C cm}^{-2}$ . It should be emphasized that such sensitivity is relatively high as compared with those for other inorganic materials, for which the value of  $E_0$  is usually  $10\text{--}10^4 \text{ mJ cm}^{-2}$  and  $D_0 > 10^4 \mu\text{C cm}^{-2}$  (see, e.g., [27], as well as [5] and references therein). The spectrum shift (figure 7(a)) has been shown to result from a change in the optical constants due to both crystallization and partial reduction of the initial anodic oxide [5].

Selective etching—chemical (in a mixture of ethanol plus 70%  $\text{HClO}_4$ ), plasma ( $\text{Ar}^+$ ), and plasma-chemical ( $\text{Cl}_2$ ,  $\text{SF}_6$ ,  $\text{CF}_4/\text{H}_2$ ,  $\text{CF}_4/\text{HF}_3$ )—of laser- and e-beam-modified films was also observed. The rate of etching of the unexposed oxide was greater than that for the exposed oxide. Using XRD (see figure 5, curve 2), it was shown that both e-beam and laser irradiation caused an irreversible crystallization of the oxide, and the observed selectivity of etching was due to the different etching rates for amorphous and crystalline regions of the oxide film. After the first etching step, if it was possible to preserve the oxide mask, the etching of the metal could occur with a high rate and selectivity. This allowed generation patterns on Si (using vanadium anodic oxide as a resist) with high resolution and smooth surfaces. Some representative SEM images of various patterns are shown in figure 8.

It has been found that the film sensitivity (i.e., the reciprocal value of  $E_0$  or  $D_0$ ), which is a key parameter for applications, also strongly depends on the electrolyte composition. It

turned out that the higher the water–borax concentration ( $C$ ), the higher the sensitivity for the ensuing films. Note that the same electrolyte composition has been found to be favourable for formation of the vanadium dioxide phase (see section 3.2 above). Moreover, in order to obtain the most sensitive films, we have used a so-called ‘non-equilibrium’ regime of anodization; that is, the films were grown at extremely high initial current densities (under volstatic conditions at  $V \leq 20$  V) for a very short time,  $\sim 1$  min. However, if one adds too much water into the electrolyte, this would also be undesirable—this will lead to the dissolution and non-uniformity of the growing AOF. Therefore it is necessary to maintain a delicate balance in water concentration in the electrolyte. For this purpose, the electrolyte composition was monitored by means of the pH and conductivity measurements. The optimal values of pH and  $\sigma$  were measured to be 6.63–6.70 and 270–350  $\mu\text{S cm}^{-1}$ , respectively, which corresponds to, approximately,  $C = 36$ –48 ml (per litre of acetone). Thus, this method has been found to be efficient enough for the control of the electrolyte composition for anodic oxidation of vanadium. Also, it has been found that salicylic and gallic acids may be apparently used instead of benzoic acid. This has been verified experimentally, and such substitution was found to enhance the electrolyte conductivity by up to an order of magnitude, improving thereby the uniformity of the oxidation process, which is especially important for a large sample area.

#### 4. Potential applications of anodic vanadium oxides

As was briefly discussed in section 1, anodic oxides, including those on vanadium, are candidate materials for a variety of technological applications, that encompass, for example, use as electrochromic and photosensitive materials, switching devices, and microsensors [3–5, 22, 26]. One more area of application is connected with the use of amorphous vanadium oxide thin films as lithography resists for nanotechnologies. This problem has already been discussed previously in a series of our publications [5, 22], and here we further elaborate on it in the light of the present results.

It should be stressed that the search for novel efficient resist materials is an important problem [28], since current organic resists are unable to meet the requirements of 100 nm and less lithography. Inorganic resists, on the other hand, seem to be promising enough and able to satisfy most of these requirements [27, 28], but research in this area has not yet resulted in a breakthrough for advanced lithographic processes. In addition, as mentioned in section 3.3, inorganic materials are usually much less sensitive than organic ones.

Transition metal oxides have demonstrated properties which put them ahead of alternative, both polymer and inorganic, resists [5]. As was discussed above, transition metals with unfilled  $d$  electron shells exhibit multiple oxidation states and form a number of oxides, which can undergo structural and phase transformations under the action of different external factors: electron and ion bombardment, laser radiation, etc. This accounts for their high sensitivity to electron-beam and photon (e.g. excimer laser DUV and EUV) radiation and permits application for both e-beam lithography and photolithography.

The material proposed, namely amorphous vanadium oxide obtained by anodic oxidation, possesses high sensitivity, i.e., low exposure thresholds—1  $\text{mJ cm}^{-2}$  for laser and 10  $\mu\text{C cm}^{-2}$  for e-beam irradiation. Also, like any other inorganic material, it possesses high absorbance of scattered radiation, and high thermal and plasma stability (as compared to polymers, such as PMMA). This allows it to be used as a single-layer resist with 0.05–0.5  $\mu\text{m}$  thickness without any significant influence of the effects which usually restrict resolution [28]—e.g., the proximity effect. In addition, since this material is amorphous, it is not limited in resolution (as an example, see figures 8(c), (d)) by the structural restrictions connected with grain boundaries and molecule dimensions in polycrystalline and polymer materials. For instance, the short-

range order region of anodic vanadium oxide films has been measured to be  $\sim 1$  nm [9] (from the position of the first maximum of curve 1 in figure 5). Physical characteristics of this material practically eliminate adverse e-beam effects [28] such as backscattering and charge accumulation. The latter is avoided due to high electrical conductivity of the vanadium oxide; in addition, vanadium dioxide undergoes an insulator-to-metal transition, and anodic vanadium oxide has been found to contain the  $\text{VO}_2$  phase. It has been shown [5, 22] that the laser- and e-beam-induced changes of the properties of amorphous vanadium oxide are associated with structural (crystallization) and chemical (in particular, the reduction  $\text{V}_2\text{O}_5 \rightarrow \text{VO}_2$ ) transformations, and non-thermal photostimulated and electrostimulated effects, including the non-equilibrium MIT in  $\text{VO}_2$ , play an important role in the mechanism of laser and e-beam modification of this material.

Furthermore, for realization of the electronic control by the MIT in vanadium dioxide<sup>1</sup>, it is necessary to obtain structures with nanodimensions and microdimensions, which would be capable of competing with conventional devices of microelectronics [29]. For this purpose, a lithographic process using the amorphous vanadium oxide could be successfully applied. That is, in this case, instead of just using the vanadium oxide as a resist for formation structures on silicon, we would use the lithography process in order to fabricate nano- $\text{VO}_2$ -based devices, such as those described in the works [26, 29].

## 5. Summary

In conclusion, we list the most important results obtained in the present study, with emphasis on the 'synthesis-properties-applications' interrelation.

- (1) Vanadium dioxide can be obtained by anodic oxidation under the following conditions: acetone-based electrolyte containing, per litre of acetone, 22 g of benzoic (or gallic, or salicylic) acid and 36–48 ml of saturated aqueous solution of borax; volstatic regime,  $V \leq 80$  V;  $t = 1$ –2 min. Other different conditions (acetic acid-based electrolyte, too high or too low water content,  $t > t_m$  or  $V > V_m$ , etc) would rather result in formation of either  $\text{V}_2\text{O}_5$ , or non-uniform films due to the effect of dissolution.
- (2) Irrespective of the oxidation conditions and phase composition, anodic oxide films on vanadium are amorphous. For amorphous vanadium dioxide, the size of the short-range order region does not exceed  $\sim 1$  nm.
- (3) The metal-insulator transition in amorphous  $\text{VO}_2$  has been studied. It is shown that the MIT in vanadium dioxide is preserved in the absence of long-range crystallographic order and that electron-electron correlations play an important role in the transition mechanism (the Mott transition [8]).
- (4) Non-equilibrium electrochemical oxidation (at a very high initial current density, under volstatic conditions at  $V \leq 20$  V, and for a relatively short time,  $\sim 1$  min) leads to the formation of metastable vanadium oxides with extremely high sensitivity to laser ( $E_0 \sim 1$  mJ cm<sup>-2</sup>) and electron-beam ( $D_0 \sim 10$   $\mu\text{C}$  cm<sup>-2</sup>) irradiation.
- (5) High sensitivity, along with the effect of selective etching and high resolution, allows the amorphous vanadium oxide films to be used as an efficient resist material for nanolithography.

<sup>1</sup> Such control could be realized, for example, in devices with injection of electrons from Si into  $\text{VO}_2$  in the structures Si-SiO<sub>2</sub>-VO<sub>2</sub> [26].

## Acknowledgment

This research was made possible in part by Award No PZ-013-02 of CRDF (USA) and the Ministry of Education (Russian Federation).

## References

- [1] Therese G H A and Kamath P V 2000 *Chem. Mater.* **12** 1195
- [2] Dell'Oka C J, Pulfrey D L and Young L 1971 *Physics of Thin Films* vol 6, ed M H Francombe and R W Hoffman (New York: Academic) pp 1–79
- Young L 1961 *Anodic Oxide Films* (New York: Academic)
- [3] Schultze J W and Lohrengel M M 2000 *Electrochim. Acta* **45** 2499
- [4] Ord J L, Bishop S D and DeSmet D J 1991 *J. Electrochem. Soc.* **138** 208
- [5] Il'in A M, Pergament A L, Stefanovich G B, Khakhaev A D and Chudnovskii F A 1997 *Opt. Spectrosc.* **82** 39
- Chudnovskii F A, Pergament A L, Schaefer D A and Stefanovich G B 1995 *J. Solid State Chem.* **118** 417
- Stefanovich G B, Pergament A L, Chudnovskii F A and Kikalov D O 1999 *Proc. SPIE* **3725** 164
- [6] Sawada T, Ishii K and Hasegawa H 1982 *Int. J. Electron.* **52** 13
- [7] Pergament A L and Stefanovich G B 1998 *Thin Solid Films* **322** 33
- [8] Mott N F 1990 *Metal-Insulator Transitions* 2nd edn (London: Taylor and Francis)
- [9] Chudnovskii F A and Stefanovich G B 1992 *J. Solid State Chem.* **98** 137
- [10] Arora M R and Kelly R 1977 *J. Mater. Sci.* **12** 1673
- Arora M R and Kelly R 1973 *J. Electrochem. Soc.* **120** 128
- [11] Mackintosh W D and Plattner H H 1976 *J. Electrochem. Soc.* **123** 523
- [12] Lewis M B and Perkins R A 1979 *J. Electrochem. Soc.* **126** 544
- [13] Keil R G and Solomon R E 1968 *J. Electrochem. Soc.* **115** 628
- Keil R G and Solomon R E 1965 *J. Electrochem. Soc.* **112** 643
- [14] Hornkjøl S and Hornkjøl I M 1991 *Electrochim. Acta* **36** 577
- [15] Al-Kharafi F M and Badawy W A 1997 *Electrochim. Acta* **42** 579
- [16] Schreckenbach J P, Witke K, Butte D and Marx G 1999 *Fresenius J. Anal. Chem.* **363** 211
- Schreckenbach J P and Strauch P 1999 *Appl. Surf. Sci.* **143** 6
- [17] Alonzo V, Darchen A, Le Fur E and Pivan J Y 2002 *Electrochem. Commun.* **4** 877
- [18] Ameer M A M and Ghoneam A A 1995 *J. Electrochem. Soc.* **142** 4082
- [19] Ellis B H, Hopper M A and De Smet D J 1971 *J. Electrochem. Soc.* **118** 860
- [20] Keil R G and Ludwig K 1971 *J. Electrochem. Soc.* **118** 864
- [21] Pelleg J 1974 *J. Less-Common Met.* **35** 299
- [22] Pergament A L, Stefanovich G B, Kazakova E L, Stefanovich D G and Velichko A A 2003 *Solid State Phenom.* **90** 97
- [23] Inaba H, Tsujimura S and Naito K 1983 *J. Solid State Chem.* **46** 162
- [24] Samsonov G V 1987 *The Oxide Handbook* (New York: Plenum)
- [25] Pergament A 2003 *J. Phys.: Condens. Matter* **15** 3217
- [26] Stefanovich G, Pergament A and Stefanovich D 2000 *J. Phys.: Condens. Matter* **12** 8837
- [27] Langheinrich W and Beneking H 1994 *Microelectron. Eng.* **23** 287
- [28] Van Zant P 1997 *Microchip Fabrication* 3rd edn (New York: McGraw-Hill)
- Merhary L, Gonsalves K E, Hu Y, He W, Huang W-S, Angelopoulos M, Bruenger W H, Dzionk C and Torkler M 2002 *Microelectron. Eng.* **63** 391
- [29] Chudnovskiy F, Luryi S and Spivak B 2002 *Future Trends in Microelectronics: the Nano Millennium; Part II: The Future Beyond Silicon* ed S Luryi, T M Xu and A Zaslavsky (New York: Wiley) pp 148–55